Separation Science and Technology
Publication details, including instructions for authors and subscription information:
http://www.informaworld.com/smpp/title~content=t713708471

Pecan Nutshell as Biosorbent to Remove Toxic Metals from Aqueous Solution

Julio C. P. Vaghetti[a]; Eder C. Lima[a]; Betina Royer[a]; Natali F. Cardoso[a]; Bruna Martins[a]; Tatiana Calvete[a]
[a] Instituto de Química, Universidade Federal do Rio Grande do Sul, CEP, Porto Alegre, RS, Brazil

To cite this Article Vaghetti, Julio C. P. , Lima, Eder C. , Royer, Betina , Cardoso, Natali F. , Martins, Bruna and Calvete, Tatiana(2009) 'Pecan Nutshell as Biosorbent to Remove Toxic Metals from Aqueous Solution', Separation Science and Technology, 44: 3, 615 — 644

To link to this Article: DOI: 10.1080/01496390802634331

URL: http://dx.doi.org/10.1080/01496390802634331

Separation Science and Technology, 44: 615–644, 2009
Copyright © Taylor & Francis Group, LLC
ISSN: 0149-6395 print/1520-5754 online
DOI: 10.1080/01496390802634331

Pecan Nutshell as Biosorbent to Remove Toxic Metals from Aqueous Solution

Julio C. P. Vaghetti, Eder C. Lima, Betina Royer, Natali F. Cardoso, Bruna Martins, and Tatiana Calvete
Instituto de Química, Universidade Federal do Rio Grande do Sul,
CEP, Porto Alegre, RS, Brazil

Abstract: In the present study we reported for the first time, the feasibility of pecan nutshell (PNS-*Carya illinoensis*) as an alternative biosorbent to remove Cr(III), Fe(III) and Zn(II) metallic ions from aqueous solutions. The ability of PNS to remove these metallic ions was investigated by using batch biosorption procedure. The effects, such as pH and the biosorbent dosage on the adsorption capacities of PNS were studied. Five kinetic models were tested, the adsorption kinetics being the better fitted one to the fractionary-order kinetic model.

The equilibrium data were fitted to Langmuir, Freundlich, Sips, and Redlich-Peterson isotherm models. Taking into account a statistical error function, the data were best fitted to Sips isotherm models. The maximum biosorption capacity of PNS were 93.01, 76.59, and 107.9 mg g^{-1} for Cr(III), Fe(III), and Zn(II), respectively.

Keywords: Biosorption, heavy metals, low-cost adsorbent, pecan nutshell

INTRODUCTION

The contamination of aquatic environment by toxic metals is of great concern due to their trends to accumulate on vital organs of humans and animals (1). In this way, the removal of toxic species from aqueous effluents before being released to the environment is required.

Received 2 April 2008; accepted 2 September 2008.

Address correspondence to Eder C. Lima, Instituto de Química, Universidade Federal do Rio Grande do Sul, Av. Bento Gonçalves 9500, Caixa Postal 15003, CEP 91501-970, Porto Alegre, RS, Brazil. Fax: +55 51 3308-7304. E-mail: eder.lima@ufrgs.br or profederlima@gmail.com

The conventional methods used to remove toxic metals from aqueous effluents include membrane filtration (2), chemical precipitation (3), ion-exchange (4), and adsorption on activated carbon (5), and silica (6–9). In the major part of the cases the use of these methods in the remediation processes is precluded due to the high costs involved (10). In this context, in the last years, several works reporting the use of alternative low cost adsorbents for toxic metal removal from aqueous solutions has been reported (10,11).

The biosorbent is a natural origin adsorbent such as microorganism (12–14), residuals of botanic materials (15–18), wastes of food industries (19,20), that are available in large amounts mainly at the proximities of the contaminated aqueous effluent, becoming this process attractive from the economical viewpoint (10,11). Because of their low cost and availability the biosorbents have successfully been used as biosorbent for removing toxic metal from aqueous media (12–20).

Pecans [*Carya illinoinensis* (Wangenh.) C. Koch], native from North America, belong to the *Juglandaceae* family which also includes walnuts (*Juglans* sp.) (21). In the south of Brazil there are extended plantation areas of the walnut tree, which were introduced by North-American immigrants in 1870 (22). The kernel of the pecan nut is largely consumed in Brazil (22); however, the nutshell is a brown by-product of difficult biodegradation. Due to the need to find new and inexpensive adsorbents for metal removal, and also to diminish the large amounts of pecan nutshell, in this work is presented an application of the use of pecan nutshell (PNS) as a biosorbent for successful removal of Cr(III), Fe(III), and Zn(II) metallic ions from aqueous solutions.

MATERIALS AND METHODS

Biosorbent Material

Pecan nuts were acquired at the local market in Porto Alegre-RS, Brazil. The weight of each seed varied between 5 and 10 g. The nutshell corresponds to approximately 49% of the walnut. About 500 g of pecan shell was washed with distilled water and further it was heated to boil in a 2 L glass beaker for 2 h. The brown aqueous solution which resulted from the pecan nutshell containing oxidized phenols (22) was discarded. Subsequently, the pecan nutshell was washed with distilled water, dried at 70°C in an air-supplied oven for 8 h. After that, the pecan nutshell was grounded in a knife-mill and subsequently sieved. The part of biosorbent with diameter of particles $\leq 250\ \mu m$ was used. The apparent density of the powder PNS was 1.30 g cm^{-3} and it presented an intense brown coloration that was assigned to poly-phenols and tannins (21,22).

The PNS biosorbent was characterized by FTIR using a Shimadzu FTIR, model 8300 (Kyoto, Japan). The spectrum was obtained with a resolution of 4 cm^{-1}, with 100 cumulative scans.

The N_2 adsorption-desorption isotherms of the biosorbent was obtained at liquid nitrogen boiling point, in a homemade volumetric apparatus (23), with a vacuum line system employing a turbomolecular Edwards vacuum pump. The pressure measurements were made with a differential pressure transducer which was coupled to a microcomputer for data acquisition. The apparatus was frequently checked with an alumina (Aldrich) standard reference (180 mesh, 3.5 nm and 200 m^2 g^{-1}). Prior to the measurements, the biosorbent sample was degassed at 200°C, in vacuum, for 30 minutes. The specific surface areas were determined from the BET (Brunauer, Emmett, and Teller) multipoint method and the pore size distribution was obtained using BJH (Barret, Joyner, and Halenda) method (23).

The biosorbent was also analyzed by scanning electron microscopy (SEM) in Jeol microscope, model JEOL JSM 6060, using an acceleration voltage of 20 kV and magnification ranging from 100 to 40,000 fold.

For determination of major mineral components of the PNS biosorbent, a digestion procedure using nitric acid and hydrogen peroxide, as described elsewhere (24), was employed. The mineral composition of the PNS biosorbent present in the digest of the biomass was determined by flame atomic absorption spectrometry using an Analyst 200 spectrometer (Perkin-Elmer).

The elemental analysis of the PNS adsorbent was carried out on a CHN Perkin–Elmer M CHNS/O Analyzer, Model 2400, after degassing treatment at 150°C. The analyses were made in triplicate.

The fiber contents of the PNS natural adsorbent was evaluated as described elsewhere (25).

The physical and chemical properties of the biosorbent are presented in Table 1.

Metallic Ion Solutions and its Determination

Stock standard solutions of metals Cr(III), Fe(III), and Zn(II), containing 5000 mg l^{-1} of each element, were prepared from $Cr_2(SO_4)_3$, $Fe_2(SO_4)_3 \cdot NH_4SO_4 \cdot 12H_2O$, $Zn(SO_4) \cdot 7H_2O$ analytical grade, furnished by Vetec (Rio de Janeiro, Brazil), by dissolving suitable amounts of these metal salts in distilled waster. Working metal solutions from 10.00 to

Table 1. Physical and chemical properties of the PNS biosorbent

Specific surface area – BET ($m^2 \cdot g^{-1}$)	100 ± 8
Average pore volume ($cm^3\,g^{-1}$)	0.080 ± 0.010
Elemental Analysis for PNS	
C (%)	48.7
H (%)	12.2
N (%)	1.39
Organic matter (%)	97.6
Carboxylic groups ($mmol \cdot g^{-1}$)	1.04
Phenolic groups ($mmol \cdot g^{-1}$)	1.11
Protein (%)	1.50
Total Fiber (%)	38.3
Ashes content (%)	1.09
Mineral composition of PNS	
Na (%)	0.114
K (%)	0.127
Ca (%)	0.124
Mg (%)	0.087
P (%)	0.287
Fe (%)	0.073
Al (%)	0.098
Mn (%)	0.036
Zn (%)	0.0047
Cu (%)	0.0020

1000.0 mg L^{-1} were prepared from suitable serial dilution of the stock solutions. The pH adjustments of the solutions were made with aliquots of 1.0 mol L^{-1} of HCl and NaOH, utilizing a pH/mV hand-held meter handylab 1 Schott (Mainz, Germany) provided with combined glass electrode model Blue-Line 23.

The transition metal ions were measured by a Perkin-Elmer Flame Atomic Absorption Spectrometer model Analyst 200 using air–acetylene flame (10:2.5 L min^{-1} for Fe and Zn and 7.6:4.3 L min^{-1} for Cr). Hollow cathode lamps of Cr ($\lambda = 357.87$ nm), Fe ($\lambda = 248.33$ nm), and Zn ($\lambda = 213.86$ nm) of the same manufacturer, were used as radiation source.

Batch Biosorption Experiments

Aliquots of 20.00 mL of 10.00–1000.0 mg L^{-1} of Cr(III), Fe(III), and Zn(II) were added to conical plastic tubes (117 mm height, 30 mm diameter) containing 20.0–300.0 mg of PNS. The flasks were capped, and placed horizontally in a Tecnal shaker model TE-240 (Piracicaba-SP, Brazil), and the system was stirred during 5 to 360 min. Afterwards, in order to separate the adsorbent from the aqueous solutions, the flasks were centrifuged using Fanem centrifuge (São Paulo-SP, Brazil) and aliquots of 1–5 mL the supernatant were properly diluted to 20.0–100.0 mL in calibrated flasks using water. The metallic ions final concentrations were determined by FAAS, after multiplying the measured concentration value found in the solution after the adsorption procedure, by the proper dilution factor.

The amount of adsorbate uptaken by the biosorbent is given by the equation 1.

$$q = \frac{(C_0 - C_f)}{m} \cdot V \tag{1}$$

Where q is the amount of metallic ion uptaken by the biosorbent (mg g^{-1}); C_0 is the initial metallic ion concentration put in contact with the adsorbent (mg L^{-1}), C_f is the metallic ion concentrations (mg L^{-1}) after the batch adsorption procedure, V is the volume of metallic ion solution (L) put in contact with the adsorbent, and m is the mass (g) of adsorbent.

Statistical Evaluation of the Kinetic and Isotherm Parameters

In this work, the kinetic and equilibrium models were fitted employing the nonlinear fitting method using the nonlinear fitting facilities of the software Microcal Origin 7.0.

In addition, the model were also evaluated by average relative error function, (9) which measures the differences of the amount of the metallic metal ion uptaken by the adsorbent predicted by the models and the actual q measured experimentally.

$$F_{error} = \sqrt{\sum_{i}^{p} \left(\frac{q_{i\,model} - q_{i\,experimental}}{q_{i\,experimental}} \right)^2 \cdot \left(\frac{1}{p-1} \right)} \tag{2}$$

Where $q_{i\ model}$ is each value of q predicted by the fitted model and $q_{i\ experimental}$ is each value of q measured experimentally, and p is the number of experiments performed.

RESULTS AND DISCUSSION

Characterization of the Biosorbent

Figure 1 shows the FTIR absorption spectra of the pecan nutshell (PNS). The band with maxima at 3405 cm^{-1} is assigned to O–H bonds (stretch) of macromolecular association (26), the band at 2925 cm^{-1} is assigned to –CH$_2$– bond (stretch) (27) and the weak band at 2854 cm^{-1} is assigned to –CH– bond of methyne group present on the PNS structure (26,27). The sharp band observed at 1708 cm^{-1} is assigned to a C=O bond of a carboxylic acid that is usually present in fiber materials containing pectin (27). The strong peak that appears at 1622 cm^{-1} is C=O stretching vibration of a carboxylic acid that exists in with intermolecular hydrogen bond (26). The sharp peak observed at 1510 cm^{-1} is assigned to C=C ring stretch of aromatic rings (26). In addition the band of 1458 cm^{-1} confirms the presence of C=C of aromatic rings (26). Several bands ranging from 1319 to 1051 cm^{-1} refer to C–O bonding of phenols (26). This splitting pattern is characteristic of several different C–O bonding of different phenols, indicating that pecan nutshell is rich in tannins, as already reported (22). From these results, it can be inferred that the metallic ions could bond to the pecan nutshell biosorbent through interaction with the active groups OH of phenolic groups (16), as well as the COOH of carboxylic acids (27). The FTIR data are also corroborated by the elemental analysis, organic matter composition, carboxylic groups and phenolic groups presented on the biosorbent (Table 1).

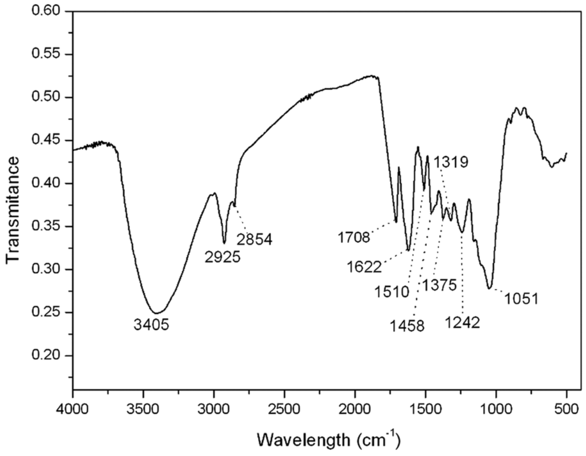

Figure 1. FTIR spectrum of pecan nutshell biosorbent.

Scanning electron microscopies of the PNS are shown in Fig. 2. The fiber material presents some fissures in its structure that allows an efficient contact of the metallic ions with the PNS, mainly at the cross section of the PNS fiber (Fig. 2a). On the other hand, on the longitudinal disposal of the fiber, few fissures can be observed (Fig. 2b) indicating that the material does not present a large amount of macropore structure. However, the best contribution of the metal ions biosorption can be attributed to micro- and meso-porous structures which cannot be visualized in the scanning electron microscopies.

The pore size distribution of the biosorbent, obtained by BJH method, is shown in Fig. 3. As can be seen, the distribution of the average

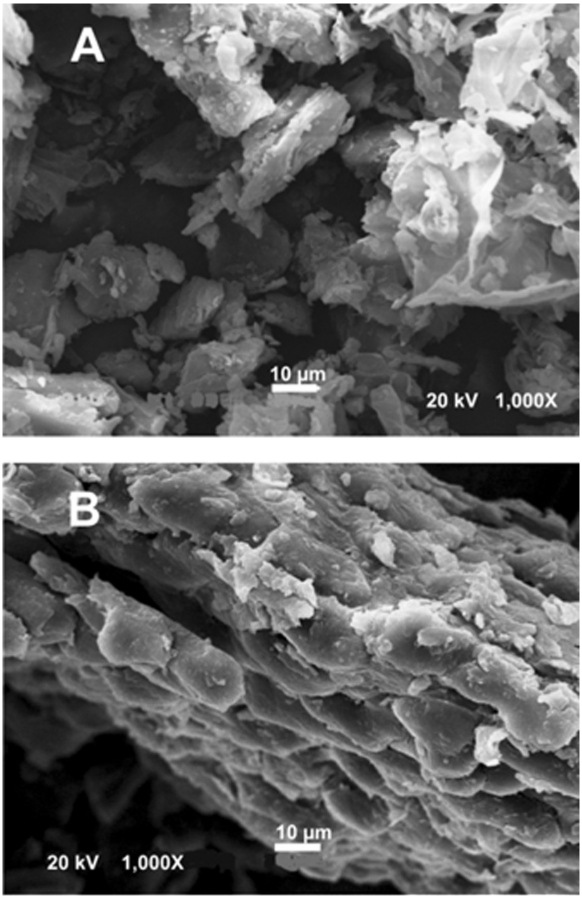

Figure 2. Scanning electron microscopy of PNS biosorbent: (A) transversal view of fiber 1,000X; (B) longitudinal view of fiber 1,000X.

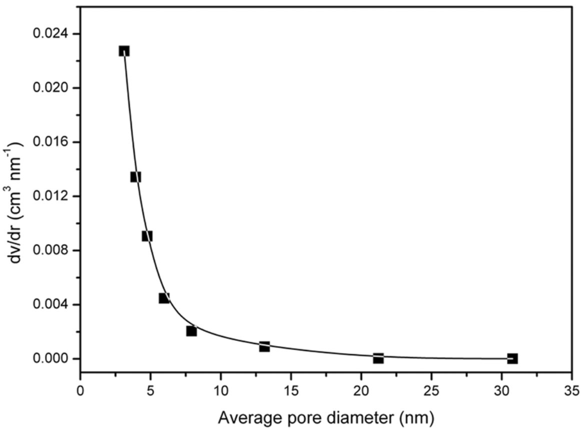

Figure 3. Pore size distribution of PNS biosorbent obtained by BJH method.

pore diameter curve presents a maximum with an average pore diameter of about 3.6 nm. The amount of pores presenting in the PW biosorbent decreases for average pore diameters ranging from 3.6 to 11 nm. On the other hand, the amount of average pores ranging from 1.0 to 3.6 nm is predominant. Therefore, this biosorbent can be considered as a mixture of micro and mesoporous materials (7,8), containing predominantly microporous, which is defined as a material that presents average diameter pore lower than 2 nm (7,8). These results are corroborated by SEM, where small amounts of macropore were visualized in the PNS fiber. Therefore the major contribution of the morphological structure of the PNS fiber for the metallic ion adsorption could be attributed mainly to micropores.

Effects of Acidity on Adsorption

One of the most important factors in adsorption studies is the effect of the acidity of the medium. Different species being adsorbed at different adsorbents will present different ranges of optimum pH region for adsorbate uptaken. The acidity of the medium affects the metal uptaken on a biosorbent because hydrogen ions can compete with metallic ions to active sites on the biosorbent surface. The effects of initial pH on the adsorption capacity of Cr(III), Fe(III), and Zn(II) ions using PNS are evaluated within the pH range of 2.0 to 8.0 (Fig. 4, at left). As can be seen, the maximum of biosorption for Cr(III) and Zn(II) takes place at pH values ranging from 5.0 to 6.0, and for Fe(III) the highest adsorption occurs at pH 4.0. These optimum acidities were in agreement with previous works for Cr(III) (20), and Zn(II) (28), and also for Fe(III)

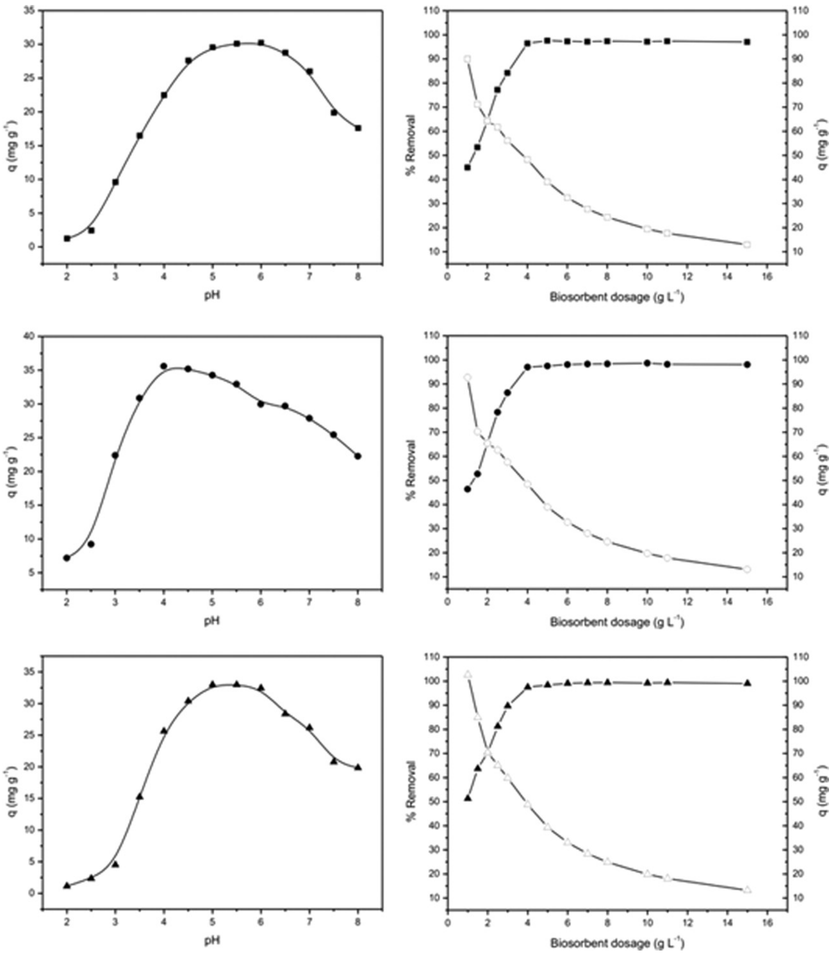

Figure 4. Left: Effect of pH on the metallic ion adsorption (100 mg L^{-1}); Right: Effect of PNS biosorbent dosage on the metallic ions (200 mg L^{-1}) removal from aqueous effluents and on the amount of metallic ion adsorbed. -■- Cr(III); -●- Fe(III); -▲- Zn(II), stands for pH and percentage of removal; -□- Cr(III); -○- Fe(III); -△- Zn(II), stands for amount adsorbed (q).

(7). For Cr(III) and Zn(II) the biosorption increased from 2.0 to 6.0. For pH values higher than 6.0, the amount of Cr(III) and Zn(II) uptaken by the biosorbent was decreased. On the other hand, for Fe(III), the adsorption increased from pH 2.0 to 4.0, and after this value, the adsorption decreased. A possible explanation to these observations for metallic ion biosorption could be attributed to the fact that at lower pH values, the dissociation of the carboxylic acids of the biosorbent leading to the formation of carboxylate groups plus H^+ will be precluded, since the pK_a of carboxylic acids ranges from 3.8 to 5.0 (29). Therefore, an increase in the pH value from 2.0 to 6.0 will lead to a remarkable increase in the amount of metallic ion biosorbed. At pH values higher than 7.0 for Cr(III) and Zn(II) and higher than 4.5 for Fe(III), the hydrolysis of metallic ions could take place (30) leading to a decrease of the biosorption process, as already observed for other biosorbents containing carboxylic acids (19,20) as well as is organically modified silica gel (7).

In order to continue this work, for Cr(III) and Zn(II) the pH value was fixed at 5.5 and for Fe(III) pH was fixed at 4.0, throughout this work.

Biosorbent Dosage

The study of biosorbent dosages for removal of Cr(III), Fe(III), and Zn(II) from aqueous solution was carried-out at different biosorbent doses (1.0–15.0 g L^{-1}) using a 200.0 mg L^{-1} of the metallic ion solutions. It was observed that almost quantitative removals of the metallic ions were attained for biosorbent dosages of at least 4.0 g L^{-1} (see Fig. 4, at right). This high metal removal efficiency means that practically all metal ions contents (200 mg L^{-1}) are adsorbed by the biosorbent and approximately no free metallic ions are left in aqueous solution. For biosorbent dosages higher than 4.0 g L^{-1} the metallic ion removal remained almost constant. Increases in the percentage of metallic ion removal with biosorbent dosages could be attributed to increases in the adsorbent surface areas, augmenting the number of adsorption sites available for adsorption. On the other hand, the increase in the biosorbent dosage promotes a decrease in the amount of metallic ion uptaken per gram of adsorbent (q_e) (see Fig. 4, at right). The decrease in q_e value may be due to the splitting effect of flux (concentration gradient) between adsorbate and biosorbent with increasing biomass concentration causing a decrease in the amount of metallic ion adsorbed per gram of biomass (31). This effect may be attributed due to the reduction in overall surface area of the biosorbent probably because of aggregation during the adsorption process, as already reported (31). In this sense, the biosorbent dosage was fixed at 4.0 g L^{-1} for all metallic ions, to continue this work.

Kinetic Studies

Adsorption kinetic study is important in the treatment of aqueous effluents as it provides valuable information on the reaction pathways and in the mechanism of adsorption reactions.

Many kinetic models were developed in order to find intrinsic kinetic adsorption constants. Traditionally, the kinetics of metal ions adsorption is described following the expressions originally given by Lagergren (32). A simple kinetic analysis of adsorption is the pseudo-first-order equation in the form

$$\frac{dq}{dt} = k_f \cdot (q_e - q_t) \tag{3}$$

Where q_t is the amount of adsorbate adsorbed at time t (mg g^{-1}), q_e is the adsorption capacity in the equilibrium (mg g^{-1}), k_f is the pseudo-first order rate constant (min^{-1}), and t is the contact time (min). The integration of equation (3) with initial conditions, $q_t = 0$ at $t = 0$, and $q_t = q_t$ at $t = t$ leads to:

$$\mathrm{Ln}\,(q_e - q_t) = \mathrm{Ln}(q_e) - k_f \cdot t \tag{4}$$

After rearranging this equation in a non-linear form the pseudo-first order kinetic equation is:

$$q_t = q_e \cdot [1 - \exp(-k_f \cdot t)] \tag{5}$$

In addition, a pseudo-second-order equation (33) based on adsorption equilibrium capacity may be expressed in the form:

$$\frac{dq_t}{dt} = k_s \cdot (q_e - q_t)^2 \tag{6}$$

Where, k_s is the pseudo-second order rate constant (g mg^{-1} min^{-1}). The integration of equation (5) with initial conditions, $q_t = 0$ at $t = 0$, and $q_t = q_t$ at $t = t$ leads to:

$$q_t = \frac{k_s \cdot q_e^2 \cdot t}{1 + q_e \cdot k_s \cdot t} \tag{7}$$

The initial sorption rate (ho, expressed in mg g^{-1} min^{-1}) can be obtained when t approaches to zero.

$$ho = k_s \cdot q_e^2 \tag{8}$$

The Elovich equation is for general application to chemisorption kinetics (34). The equation has been applied satisfactorily to some chemisorption processes and has been found to cover a wide range of slow adsorption rates. The same equation is often valid for systems in which the adsorbing surface is heterogeneous, and is formulated as:

$$\frac{dq_t}{dt} = \alpha \exp(-\beta q_t) \tag{9}$$

Integrating this equation for the boundary conditions, $q_t = 0$ at $t = 0$ and $q_t = q_t$ for $t = t$, it gives:

$$q_t = \frac{1}{\beta} Ln(t + t_o) - \frac{1}{\beta} \cdot Ln(t_o) \tag{10}$$

where α is the initial adsorption rate ($mg\,g^{-1}\,min^{-1}$) and β is related to the extent of surface coverage and the activation energy involved in chemisorption ($g\,mg^{-1}$) and $t_o = 1/\alpha\beta$.

If t is much larger than to, the kinetic equation can be simplified as

$$q_t = \frac{1}{\beta} Ln(\alpha \cdot \beta) + \frac{1}{\beta} Ln(t) \tag{11}$$

Despite the pseudo-first and pseudo-second order kinetic models being used for most adsorption kinetic works, determination of some kinetic parameters, as possible changes of the adsorption rates in function of the initial concentration and the adsorption time, as well as the determination of fractionary kinetic orders, still lacks in the kinetic adsorption models (35). In this way, an alternative Avrami kinetic equation, in order to find a good experimental and calculated data correlation, was early proposed (35). The adsorption should be visualized now using Avrami's exponential function, which is an adaptation of kinetic thermal decomposition modeling (35).

$$\alpha = 1 - \exp[-(k_{AV} \cdot t)]^n \tag{12}$$

where α is adsorption fraction (q_t/q_e) at time t, k_{AV} is the Avrami kinetic constant (min^{-1}), and n is a fractionary reaction order which can be related, to the adsorption mechanism (35).

By inputting the α in equation 12, the Avrami kinetic equation could be written as:

$$q_t = q_e \cdot \{1 - \exp[-(k_{AV} \cdot t)]^n\} \tag{13}$$

For describing the adsorption of Cr(III), Fe(III), and Zn(II) on PNS biosorbent the four kinetic models depicted above were fitted (Fig. 5). The kinetic parameters of the fitted models are presented on Table 2.

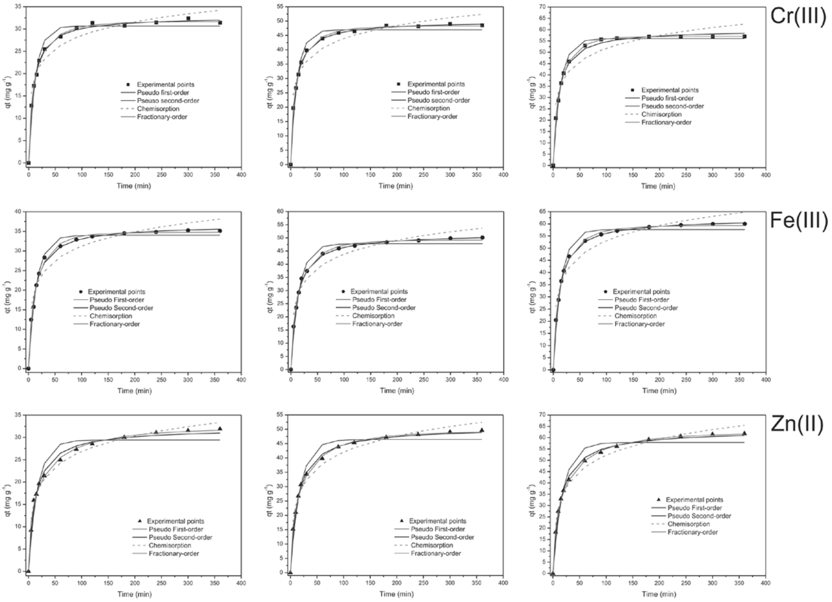

Figure 5. Non-linear kinetic models for the adsorption of Cr(III), Fe(III), and Zn(II) using PNS as biosorbent. -■- Cr(III); -●- Fe(III); -▲- Zn(II).

As can be seen, the Avrami fractionary kinetic order and pseudo second-order kinetic models, in decreasing ranking are suitably fitted, presenting low error function values and also high R^2 values, for the three initial concentration levels of the metallic ions employed. How lower is the error function, lower will be the difference of the q calculated by the model from the q experimentally measured (9). It should be stressed that only the analysis of R^2 values to the establishment of a given model is not enough, because the error function evaluates the differences associated with each individual point fitted by the model in relation to each experimental point measured. On the other hand the R^2 value measures the differences associated with each individual point in relation to the average fitted curve (9). This could be visualized by seeing the R^2 and the F_{error} values of the fractionary order kinetic model and the pseudo-second order kinetic model, when the initial concentration of Cr(III) was 200.0 mg L^{-1} as well as the Zn(II) was 100.0 mg L^{-1}. In the first case, the R^2 value of pseudo-second order ($R^2 = 0.9989$) was slightly better than the fractionary order model ($R^2 = 0.9985$); however, the F_{error} value for the fractionary order kinetic model (0.01415) was better than the pseudo-second order kinetic model (0.01771). In the second case,

Table 2. Kinetic parameters for Cr(VI), Fe(III) and Zn(II) using PNS as biosorbent. Conditions: temperature was fixed at 25°C, pH 5.5 for Cr(III) and Zn(II) and at 4.0 for Fe(III), biosorbent dosage 4.0 g L^{-1}

	C_o (mg L^{-1})								
	Cr(III)			Fe(III)			Zn(II)		
	100.0	200.0	300.0	100.0	200.0	300.0	100.0	200.0	300.0
Fractionary order									
k_{AV} (min^{-1})	0.0693	0.0732	0.0661	0.0601	0.0569	0.0589	0.0394	0.0423	0.0386
q_e (mg g^{-1})	31.7	48.3	57.0	34.7	49.2	59.3	32.1	49.2	62.1
n	0.620	0.631	0.730	0.719	0.681	0.677	0.533	0.604	0.581
R^2	0.9979	0.9985	0.9995	0.9958	0.9973	0.9984	0.9944	0.9979	0.9989
F_{error}	0.0165	0.0142	0.0129	0.0367	0.0244	0.0189	0.0634	0.0264	0.0274
Pseudo-first order									
k_f (min^{-1})	0.0751	0.0782	0.0694	0.0649	0.0635	0.0652	0.0575	0.0543	0.0523
q_e (mg g^{-1})	30.7	47.0	56.0	34.0	47.8	57.7	29.4	46.4	57.9
R^2	0.9761	0.9805	0.9895	0.9865	0.9843	0.9849	0.9546	0.9719	0.9666
F_{error}	0.0855	0.0759	0.0674	0.0765	0.0719	0.0727	0.106	0.0984	0.107
Pseudo-second order									

k_s (g mg^{-1} min^{-1})	0.00351	0.00240	0.00173	0.00256	0.00175	0.00151	0.00244	0.00145	0.00111
q_e (mg g^{-1})	32.7	50.1	59.9	36.6	51.6	62.1	32.1	50.7	63.4
ho (mg g^{-1} min^{-1})	3.76	6.02	6.22	3.43	4.65	5.83	2.51	3.73	4.46
R^2	0.9968	0.9989	0.9969	0.9954	0.9988	0.9993	0.9917	0.9977	0.9969
F_{error}	0.0278	0.0177	0.0244	0.0430	0.0185	0.0169	0.0433	0.0334	0.0354
Chemisorption									
α (mg g^{-1} min^{-1})	29.7	51.3	40.2	18.2	22.9	30.8	10.1	14.4	16.5
β (g mg^{-1})	0.228	0.152	0.119	0.186	0.130	0.110	0.197	0.123	0.0972
R^2	0.9675	0.9661	0.952	0.9580	0.9673	0.9665	0.9885	0.984	0.9886
F_{error}	0.0820	0.0874	0.109	0.105	0.101	0.0982	0.0826	0.0334	0.0614
Intra-particle diffusion									
ki (mg g^{-1} min$^{-0.5}$)*	1.08	1.04	1.91	0.778	0.742	0.805	1.09	1.64	2.20

*Second stage.

the F_{error} values evaluated better the pseudo-second order kinetic model in relation to the fractionary kinetic model, although the simple analysis of R^2 values were in opposite directions. These results reinforce the need of using a statistical error function to better evaluate the adsorption models, as previously reported (9).

Additionally, it was verified that the q_e values found in the fractionary order as well as in the pseudo-second order kinetic models were in good agreement with the experimental q_e values. These results indicate that both the fractionary order and the pseudo-second order kinetic models should be taken into account for explaining the adsorption process of Cr(III), Fe(III), and Zn(II) uptaken by the PNS biosorbent.

By analyzing the values of the kinetic parameters depicted in Table 2, it should be mentioned that the k_{AV} values are much better for the evaluation of the kinetic process than the pseudo-second order kinetic constant (k_S), since the values of the Avrami's constant does not depend on the initial concentration of the adsorbate, since its unit is min^{-1}. On the other hand, the k_S values strongly depend on the initial concentration, since its units is $g\ mg^{-1} min^{-1}$. Observing the data reported in Table 2, the percentage of variation of k_{AV} was lower than 10% for the three metallic ions using three different initial concentration levels. On the other hand, the percentage of variation of k_S was up to 120%, when the initial concentration levels of the metallic ions were increased from $100.0\,mg\,L^{-1}$ to $300.0\,mg\,L^{-1}$. Therefore, the fractionary kinetic model provides a constant rate parameter which is much better for comparison of different kinetic constants, using different adsorbates and adsorbents.

Taking into account that the kinetic results fitted very well to the fractionary kinetic model, and fairly good to pseudo second order kinetic models (see Table 2 and Fig. 5), the intra-particle diffusion model (36), was plotted in order to verify the influence of mass transfer resistance on the binding of Cr(III), Fe(III), and Zn(II) to the PNS biosorbent (see Table 2 and Fig. 6).

The possibility of intra-particle diffusion resistance affecting adsorption was explored using the intra-particle diffusion model as (36):

$$q_t = k_{id} \cdot \sqrt{t} + C \tag{14}$$

Where k_{id} is the intra-particle diffusion rate constant ($mg\,g^{-1}\,min^{-0.5}$), and C is a constant related with the thickness of the boundary layer ($mg\,g^{-1}$).

Thus, the intra-particle diffusion constant, k_i ($mg\,g^{-1}\,min^{-0.5}$), can be obtained from the slope of the plot of q_t (uptake at any time, $mg\,g^{-1}$)

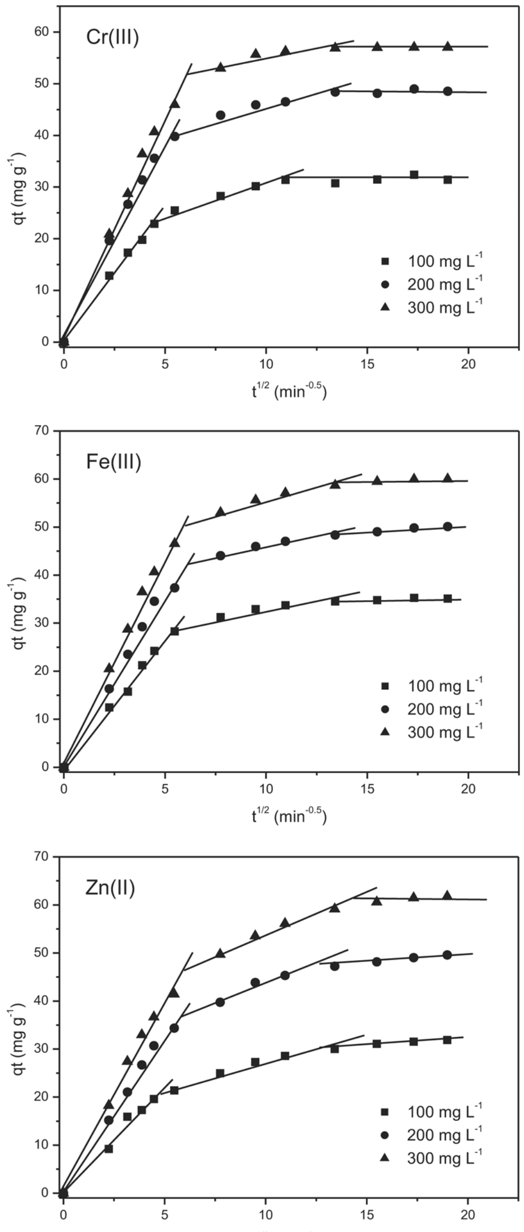

Figure 6. Intra-particle diffusion kinetic model for the adsorption of Cr(III), Fe(III), and Zn (II).

versus the square root of time (Fig. 6). If this plot passes through the origin, then intra-particle diffusion is the rate controlling step. Figure 6 shows the plots of q_t versus $t^{1/2}$, with multi-linearity for the three metallic ions chosen, which implies that the adsorption process involves more than one kinetic stage (or sorption rates) (37).

For instance, the PNS exhibited three stages, which can be attributed to each linear portion of the figure. The first linear portion was attributed to the diffusional process of metallic ions to the PNS biosorbent surface (37); hence, was the fastest sorption stage. The second portion, ascribed to intra-particle diffusion, was a delayed process. The third stage may be regarded as the diffusion through smaller pores, which is followed by the establishment of equilibrium. The presence of microporous on the PNS biosorbent (see Fig. 3) corroborates with this last stage of the intra-particle diffusion process.

Desorption Experiments

Desorption experiments were carried-out in order to verify the possible mechanism of adsorption of Cr(III), Fe(III), and Zn(II) on PNS. Batch desorption studies were carried out by agitating 20.0 mL of 200.0 mg L^{-1} metallic ion solutions with 80.0 mg of PNS (biosorbent dosage of 4.0 g L^{-1}) for 150 min. The remaining liquid phase was separated from the solid phase, and the metallic loaded adsorbents, were first washed with water for removing non-adsorbed metallic ions. Then, metallic loaded biosorbents were agitated with 25.0 ml of aqueous solutions (0.050–0.80 mol L^{-1} HCl; 0.050–0.80 mol L^{-1} HNO_3; 0.010 – 0.50 mol L^{-1} KCl; and 0.050–0.15 mol L^{-1} NaOH) up to 1 h (see Fig. 7). It was observed that NaOH did not lead to any removal of the metallic ions loaded biosorbents after 1 h of contact time (see Fig. 7). In addition, the desorption experiments carried-out with KCl promoted a slight regeneration of the metal loaded PNS biosorbent (<25%) (see Fig. 7). The best recovery results were achieved by using HCl and HNO_3 (see Fig. 7). These results indicate that the metallic ions should interact with the carboxylic acid and phenolic groups present of the PNS biosorbent, as described in the Scheme 1.

In the first step, the acidity of the medium should be adjusted by keeping the pH ranging from 4.0 to 6.0, in order to the release of H^+ from the PNS biosorbent. In the second step, the metal uptake by the PNS fiber took place. In the third step, the release of metallic ions from the loaded biosorbents occur by the addition of HNO_3 and/or HCl, regenerating the biosorbent.

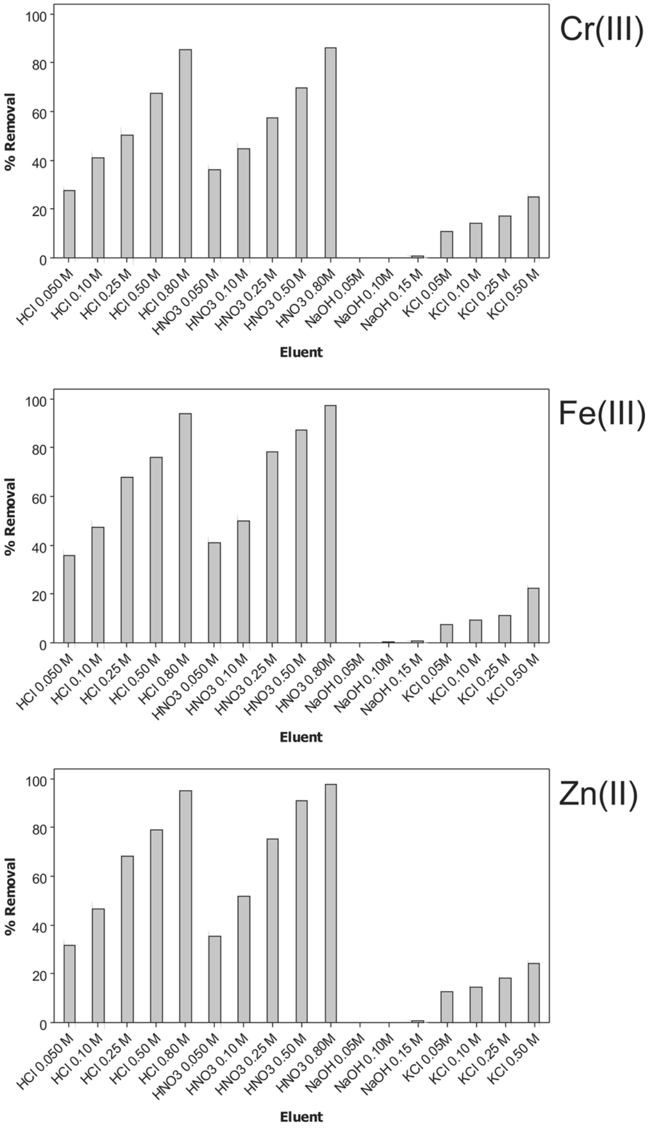

Figure 7. Desorption of metallic ions loaded on PNS biosorbent.

The regenerated biosorbent was again employed for metal uptake, obtaining at least 80% of the initial adsorption capacity of the original biosorbent, for the three chosen metallic ions.

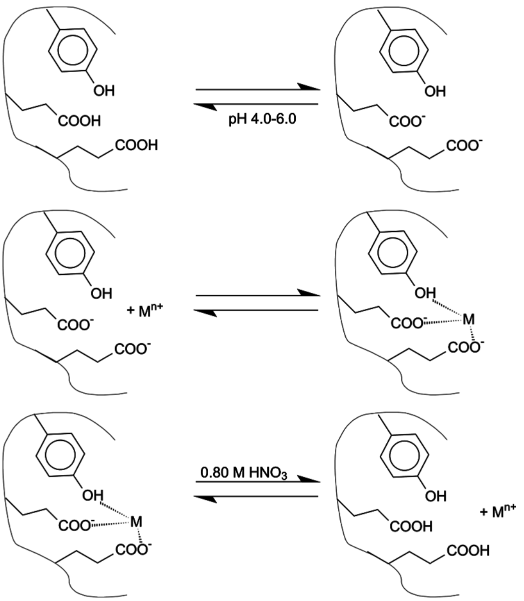

Scheme 1. Mechanism of adsorption and desorption of metallic ions by PNS.

Equilibrium Studies

An adsorption isotherm describes the relationship between the amount of adsorbate uptaken by the adsorbent and the adsorbate concentration remaining in solution. There are many equations for analyzing the experimental adsorption equilibrium data. The equation parameters of these equilibrium models often provide some insight into both the adsorption mechanism and the surface properties and affinity of the adsorbent. In this work, the Langmuir (38), Freundlich (39), Sips (40), and Redlich and Peterson (41) isotherm models were tested.

Langmuir Isotherm Model

The Langmuir (38) isotherm is based on the following assumptions:

- adsorbates are chemically adsorbed at a fixed number of well-defined sites;
- each site can only hold one adsorbate specie;
- all sites are energetically equivalent;
- There are no interactions between the adsorbate species.

The Langmuir isotherm equation is:

$$q_e = \frac{Q_{max} \cdot K_L \cdot C_e}{1 + K_L \cdot C_e} \tag{15}$$

where, C_e is the supernatant concentration after the equilibrium of the system (mg l^{-1}), K_L the Langmuir affinity constant (L mg^{-1}), and Q_{max} is the maximum adsorption capacity of the material (mg g^{-1}) assuming a monolayer of adsorbate uptaken by the adsorbent.

Freundlich Isotherm

The Freundlich (39) isotherm model is an exponential equation and therefore assumes that the concentration of the adsorbate on the adsorbent surface increases with the adsorbate concentration. Theoretically, using this expression, an infinite amount of adsorption can occur. The equation is widely applied in heterogeneous systems.

The Freundlich isotherm model is:

$$q = K_F \cdot Ce^{1/n} \tag{16}$$

Where K_F is the Freundlich constant related with the adsorption capacity [mg g^{-1} (mg $L^{-1})^{-1/n}$] and n is the Freundlich exponent (dimensionless).

Sips Isotherm Model

This model is an empirical model and it consists of the combination of the Langmuir and Freundlich isotherm type models. The Sips (40) model takes the following form:

$$q = \frac{Q_{max} \cdot K_S \cdot Ce^{1/n}}{1 + K_S \cdot Ce^{1/n}} \tag{17}$$

Where K_S is the Sips constant related with affinity constant (mg $L^{-1})^{-1/n}$ and Q_{max} is the Sips maximum adsorption capacity (mg g^{-1}).

At low adsorbate concentrations it effectively reduces to a Freundlich isotherm, while at high adsorbate concentrations it predicts a monolayer adsorption capacity characteristic of the Langmuir isotherm.

Redlich-Peterson Isotherm Model

This is an empirical equation that describes an equilibrium isotherm (41).

$$q = \frac{K_{RP} \cdot Ce}{1 + a_{RP} \cdot Ce^g} \quad \text{where } g \leq 1 \tag{18}$$

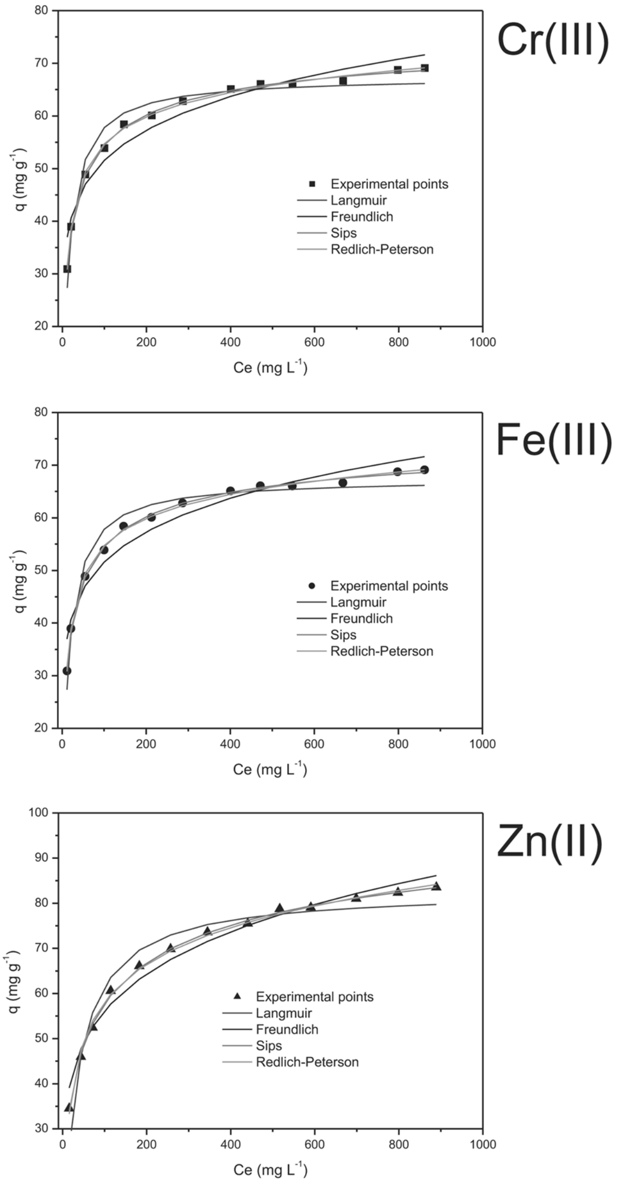

Figure 8. Adsorption isotherm models for Cr(III), Fe(III), and Zn(II) adsorption from aqueous solutions on PNS biosorbent using batch adsorption procedure at 25°C, biosorbent dosage of 4.0 g L^{-1}, pH fixed at 5.5 for Cr(III) and Zn(II) and using a contact time of 120 min.

Where K_{RP} and a_{RP} are Redlich-Peterson constants, with the respective units: L g^{-1} and $(mg\,L^{-1})^{-g}$ and g is the Redlich-Peterson exponent (dimensionless), whose value should be ≤ 1. This equation reduces to a linear isotherm in the case of low surface coverage ($g = 0$) and to a Langmuir isotherm when $g = 1$.

The isotherms of adsorption of Cr(III), Fe(III), and Zn(II) on the PNS adsorbent were performed using the best experimental conditions described previously (see Fig. 8).

The data of the fitted models are presented in Table 3. Based on the F_{error} values, the best isotherm model fitted was the Sips for Cr(III) and Zn(II), and Redlich-Peterson for Fe(III), that presented the lowest values for F_{error}, which means that the q fitted by the isotherm model were close to the q measured experimentally. The differences of the F_{error} values between the Sips and Redlich-Peterson isotherm models were not so

Table 3. Isotherm parameters for Cr(III), Fe(III), and Zn(II) biosorption, using PNS as biosorbent. Conditions: temperature was fixed at 25°C, biosorbent dosage 4.0 g L^{-1}, contact time was fixed at 3 h, and pH was fixed at 5.5 for Cr(III) and Zn(II) and at 4.0 for Fe(III)

	Cr(III)	Fe(III)	Zn(II)
Langmuir			
Q_{max} ($mg\,g^{-1}$)	77.5	67.4	82.8
K_L ($L\,mg^{-1}$)	0.0263	0.0602	0.0288
R^2	0.9704	0.9605	0.9468
F_{error}	0.103	0.0503	0.0817
Freudlich			
K_F ($mg\cdot g^{-1}\cdot(mg\cdot L^{-1})^{-1/n}$)	17.3	25.5	22.8
n	4.36	6.56	5.11
R^2	0.9617	0.9468	0.9774
F_{error}	0.122	0.0674	0.0476
Sips			
Q_{max} ($mg\,g^{-1}$)	93.0	76.6	108
K_S ($(mg\,L^{-1})^{-1/n}$)	0.0774	0.171	0.117
n	1.63	1.72	2.01
R^2	0.9987	0.9979	0.9986
F_{error}	0.0118	0.0107	0.0103
Redlich-Peterson			
K_{RP} ($L\cdot g^{-1}$)	4.05	7.03	6.31
a_{RP} $(mg\cdot L^{-1})^{-\beta}$	0.118	0.169	0.181
β_{RP}	0.876	0.924	0.868
R^2	0.9976	0.9979	0.9966
F_{error}	0.0191	0.00926	0.0179

remarkable, indicating that these two isotherm models were suitably fitted for Cr(III), Fe(III), and Zn(II). On the other hand, the Langmuir and Freundlich isotherm models presented high F_{error} values, besides presenting low R^2 values, indicating that these models were not suitably fitted for Cr(III), Fe(III), and Zn(II) as adsorbates, using PNS as a biosorbent. The importance of using error functions to evaluate the isotherm models should be highlighted. For Fe(III), although the R^2 value of the Sips (R^2 0.9979) was exactly the same value obtained for the Redlich-Peterson isotherm model, the F_{error} values for the Sips isotherm model (F_{error} 0.01071) was a little bit worse than the Redlich-Peterson isotherm model (F_{error} 0.009256). The error function evaluates how much each

Table 4. Comparison of maxima adsorption capacities of Cr(III), Fe(III), and Zn(II) on different adsorbents

	Adsorption capacity (mg g^{-1})			
Adsorbent	Cr(III)	Fe(III)	Zn(II)	Ref
10-Amine-4-azadecylsilica gel	—	55.2	—	7
7-Amine-4-azaheptylsilica gel	—	39.7	—	7
Aniline grafted silica gel	16.0	—	—	9
Yellow passion-fruit shell	85.1	—	—	20
Chemically treated newspaper pulp	—	—	26.3	28
Kaolinite	3.44	—	—	42
Dried green alga	10.6	—	—	43
Activated carbon from alga	112	—	—	44
Aspergillus niger fungal biomass	11.6	—	—	44
Fresh water green algae *spirogyra* spp.	30.2	—	—	45
Lignite	—	11.9	—	46
Pyrocatechol immobilized cellulose	—	6.10	—	47
Raw clinoptilolite	—	98.0	—	48
Pretreated clinoptilolite	—	104	—	48
Clinoptilolite from Thrace	—	—	71.3	49
Clinoptilolite–mixed with Fe oxide	—	—	94.8	49
Penicillium italicum – loaded on Sepabeads	—	12.5	—	50
Natural clay	—	—	80.7	51
Acid-treated coconut shell carbon	—	—	60.4	52
Chitosan coated on coconut shell carbon	—	—	50.9	52
Chitosan coated on acid-treated coconut shell	—	—	45.1	52
Mesoporous chemically modified silica-gel	—	—	34.7	53
Orange peel	—	—	79.1	54
Cyanobacterium *Aphanothece halophytica*	—	—	133	55
Pecan nutshell	93.0	76.6	108	This work

individual q fitted by the isotherm model differs from the q measured experimentally.

Comparison of Different Adsorbents for Cr(III), Fe(III), and Zn(II) Adsorption

In Table 4 is presented a comparison of several adsorbents employed for Cr(III), Fe(III), and Zn(II) adsorption. As can be seen from Table 4, the PNS biosorbent employed in this work presents very high adsorption capacities for Cr(III), Fe(III), and Zn(II) when compared with several different adsorbents. For Cr(III), from 7 different adsorbents, PNS presents a higher sorption capacity than 6; for Fe(III) from 7 different adsorbents, PNS is better than 5; and for Zn(II) from 10 different adsorbents the PNS is better than 9. It should be stressed that Table 4 is not a comprehensive table, where there is a possibility of a nonlisted adsorbent present a higher sorption capacity than those reported in this paper. On the other hand, the outstanding sorption capacities for Cr(III), Fe(III), and Zn(II) places pecan nutshell as one of the best adsorbents for metallic ion removal from aqueous solutions.

CONCLUSION

Pecan nutshell (PNS) is a very good alternative biosorbent for removal of Cr(III), Fe(III), and Zn(II) from aqueous solutions. The biosorbent was used without any chemical treatment presenting biosorption capacities of 93.01, 76.59, and 107.9 $\mathrm{mg\,g^{-1}}$ for Cr(III), Fe(III), and Zn(II), respectively. In this way, the use of pecan nutshell as a biosorbent can be interesting at the commercial viewpoint because of its low preparation cost and large availability in South Brazil.

The PNS biosorbent was characterized by FTIR spectroscopy indicating the presence of phenolic, O–H groups, and carboxylic groups (COOH). These data were also confirmed by conventional titrations where the amounts of phenolic and carboxylic groups measured were 1.11 and 1.04 $\mathrm{mmol\,g^{-1}}$, respectively, in PNS biosorbent.

The pore size distribution curve and SEM of the biosorbent employed, indicated that PNS could be considered mixtures of microporous and mesoporous, with the predominance of micropore structure.

The adsorption of the metallic ions depended on pH and shaking contact time. The optimum pH for the adsorption of the metallic ion was 5.5 for Cr(III) and Zn(II) and 4.0 for Fe(III) and the shaking contact time necessary for reaching the equilibrium was 120 min.

There are several indicatives (fractionary kinetic model, pseudo-second order kinetic model, intra-particle diffusion model, and desorption experiments) that the mechanism of biosorption of all metallic ions by PNS should be an interaction of the carboxylic and phenolic groups of PNS with the metallic ion at pH ranging from 4.0 to 6.0 (see Scheme 1).

About 95–98% of the metallic ions loaded biosorbent were regenerated, using $0.80\,\mathrm{mol\,L^{-1}}$ of HCl or HNO_3. The regenerated biosorbent could be employed again for metal uptake, keeping at least 80% of the initial sorption capacity. These results reinforce that the use of pecan nutshell could be a good alternative for Cr(III), Fe(III), and Zn(II) removal from the aqueous solution.

ACKNOWLEDGEMENTS

The authors are grateful to Ministério de Ciência e Tecnologia (MCT), to Conselho Nacional de Desenvolvimento Científico e Tecnológico (CNPq), and to Coordenação de Aperfeiçoamento de Pessoal de Nível Superior (CAPES) for financial support and fellowships. We are grateful to Centro de Microscopia Eletrônica (CME-UFRGS) for the use of the SEM microscope. We would also like to thank Perkin Elmer for donating impact beads utilized in the nebulizer of the Analyst 200 spectrometer.

REFERENCES

1. Yu, M.H. (2005) *Environmental Toxicology-Biological and Health Effects of Pollutants;* 2nd Ed.; CRC Press: Boca Raton.
2. Khedr, M.G. (2008) Membrane methods in tailoring simpler, more efficient, and cost effective wastewater treatment alternatives. *Desalination*, *222*: 135.
3. González-Muñoz, M.J.; Rodríguez, M.A.; Luque, S.; Álvarez, J.R. (2006) Recovery of heavy metals from metal industry waste waters by chemical precipitation and nanofiltration. *Desalination*, *200*: 742.
4. Pehlivan, E.; Altun, T. (2007) Ion-exchange of Pb^{2+}, Cu^{2+}, Zn^{2+}, Cd^{2+}, and Ni^{2+} ions from aqueous solution by Lewatit CNP. *J. Hazard. Mater.*, *140*: 299.
5. Santhy, K.; Selvapathy, P. (2004) Removal of heavy metals from wastewater by adsorption on coir pith activated carbon. *Sep. Sci. Technol.*, *39*: 3331.
6. Vaghetti, J.C.P.; Zat, M.; Bentes, K.R.S.; Ferreira, L.S.; Benvenutti, E.V.; Lima, E.C. (2003) 4-Phenylenediaminepropylsilica xerogel as a sorbent for copper determination in waters by slurry-sampling ETAAS. *J. Anal. At. Spectrom.*, *18*: 376.
7. Passos, C.G.; Ribaski, F.; Simon, N.M.; dos Santos-Junior, A.A.; Vaghetti, J.C.P.; Benvenutti, E.V.; Lima, E.C. (2006) Use of statistical design of

experiments to evaluate the sorption capacity of 7-amine-4-azahepthylsilica and 7-amine-4-azahepthylsilica for Cu(II), Pb(II) and Fe(III) adsorption. *J. Colloid Interface Sci.*, *302*: 396.

8. Arenas, L.T.; Lima, E.C.; dos Santos-Junior., A.A.; Vaghetti, J.C.P.; Costa, T.M.H.; Benvenutti, E.V. (2007) Use of statistical design of experiments to evaluate the sorption capacity of 1,4-diazoniabicycle[2.2.2]octane/silica chloride for Cr(VI) adsorption. *Colloids Surf. A*, *297*: 240.
9. Jacques, R.A.; Bernardi, R.; Caovila, M.; Lima, E.C.; Pavan, F.A.; Vaghetti, J.C.P.; Airoldi, C. (2007) Removal of Cu(II), Fe(III) and Cr(III) from aqueous solution by aniline grafted silica gel. *Sep. Sci. Technol.*, *42*: 591.
10. Babel, S.; Kurniawan, T.A. (2003) Low-cost adsorbents for heavy metals uptake from contaminated water: A review. *J. Hazard. Mater.*, *97*: 219.
11. Kurniawan, T.A.; Chan, G.Y.S.; Lo, W.H.; Babel, S. (2006) Comparisons of low-cost adsorbents for treating wastewaters laden with heavy metals. *Sci. Total Environ.*, *366*: 409.
12. Zouboulis, A.I.; Matis, K.A.; Lazaridis, N.K. (2001) Removal of metal ions from simulated wastewater by *saccharomyces* yeast biomass: Combining biosorption and flotation processes. *Sep. Sci. Technol.*, *36*: 349.
13. Parvathi, K.; Nagendran, R. (2007) Biosorption of chromium from effluent generated in chrome-electroplating unit using *Saccharomyces cerevisiae*. *Sep. Sci. Technol.*, *42*: 625.
14. Ghimire, K.N.; Inoue, K.; Ohto, K.; Hayashida, T. (2007) Adsorptive separation of metallic pollutants onto waste seaweeds, Porphyra Yezoensis and Ulva Japonica. *Sep. Sci. Technol.*, *42*: 2003.
15. Brasil, J.L.; Ev, R.R.; Milcharek, C.D.; Martins, L.C.; Pavan, F.A.; dos Santos-Junior., A.A.; Dias, S.L.P.; Dupont, J.; Noreña, C.P.Z.; Lima, E.C. (2006) Statistical design of experiments as a tool for optimizing the batch conditions to Cr(VI) biosorption on Araucaria angustifolia wastes. *J. Hazard. Mater.*, *133*: 143.
16. Lima, E.C.; Royer, B.; Vaghetti, J.C.P.; Brasil, J.L.; Simon, N.M.; dos Santos-Junior, A.A.; Pavan, F.A.; Dias, S.L.P.; Benvenutti, E.V.; da Silva, E.A. (2007) Adsorption of Cu(II) on Araucaria angustifolia wastes: Determination of the optimal conditions by statistic design of experiments. *J. Hazard. Mater.*, *140*: 211.
17. Machado, R.M.; Correia, M.J.N.; Carvalho, J.M.R. (2003) Integrated process for biosorption of copper from liquid effluents using grape stalks. *Sep. Sci. Technol.*, *28*: 2237.
18. Javed, M.A.; Bhatti, H.N.; Hanif, M.A.; Nadeem, R. (2007) Kinetic and equilibrium modeling of Pb(II) and Co(II) sorption onto rose waste biomass. *Sep. Sci. Technol.*, *42*: 3641.
19. Pavan, F.A.; Lima, I.S.; Lima, E.C.; Airoldi, C.; Gushikem, Y. (2006) Use of ponkan mandarin peels as biosorbent for toxic metals uptake from aqueous solutions. *J. Hazard. Mater.*, *137*: 527.
20. Jacques, R.A.; Lima, E.C.; Dias, S.L.P.; Mazzocato, A.C.; Pavan, F.A. (2007) Yellow passion-fruit shell as biosorbent to remove Cr(III) and Pb(II) from aqueous solution. *Sep. Purif. Technol.*, *57*: 193.

21. Villarreal-Lozoya, J.E.; Lombardini, L.; Cisneros-Zevallos, L. (2007) Phytochemical constituents and antioxidant capacity of different pecan [Carya illinoinensis (Wangenh.) K. Koch] cultivars. *Food Chem.*, *102*: 1241.
22. Brasil, J.L.; Vaghetti, J.C.P.; Royer, B.; dos Santos-Junior, A.A.; Simon, N.M.; Pavan, F.A.; Dias, S.L.P.; Lima, E.C. (2007). Statistical design of experiments as a tool for optimizing the batch conditions of Cu(II) biosorption using pecan nutshells as biosorbent. *Quim. Nova*, *30*: 548.
23. Passos, C.G.; Lima, E.C.; Arenas, L.T.; Simon, N.M.; da Cunha, B.M.; Brasil, J.L.; Costa, T.M.H.; Benvenutti, E.V. (2008) Use of 7-amine-4-azahepthylsilica and 10-amine-4-azadecylsilica xerogels as adsorbent for Pb(II). Kinetic and equilibrium study. *Colloids Surf. A*, *316*: 297.
24. Lima, E.C.; Krug, F.J.; Ferreira, A.T.; Barbosa-Junior., F. (1999) Tungsten-rhodium permanent chemical modifier for cadmium determination in fish slurries by electrothermal atomic absorption spectrometry. *J. Anal. At. Spectrom.*, *14*: 269.
25. Prosky, L.; Asp, N.G.; Schweizer, T.; de Vries, J.W.; Furda, I. (1992) Determination of insoluble and soluble dietary fiber in food and food products: Collaborative study. *J. AOAC Inter.*, *75*: 360.
26. Pavia, D.L.; Lampman, G.M.; Kriz, G.S. (1996) *Introduction to Spectroscopy;* 2nd Ed.; Saunders Golden Sunburst Series: New York.
27. Pavan, F.A.; Lima, E.C.; Dias, S.L.P.; Mazzocato, A.C. (2008) Methylene blue biosorption from aqueous solutions by yellow passion fruit waste. *J. Hazard. Mater.*, *150*: 703.
28. Chakravarty, S.; Bhattacharjee, S.; Gupta, K.K.; Singh, M.; Chaturvedi, H.T.; Maity, S. (2007) Adsorption of zinc from aqueous solution using chemically treated newspaper pulp. *Bioresour. Technol.*, *98*: 3136.
29. Roberts, J.D.; Caserio, M.C. (1977) *Basic Principles of Organic Chemistry;* 2nd Ed.; W.A. Benjamin: London.
30. Kolthoff, I.M.; Sandell, E.B.; Meehan, E.J.; Bruckentein, S. (1969) *Quantitative Chemical Analysis;* 4th Ed.; The Macmillan Company: Lodon.
31. Lima, E.C.; Royer, B.; Vaghetti, J.C.P.; Simon, N.M.; da Cunha, B.M.; Pavan, F.A.; Benvenutti, E.V.; Veses, R.C.; Airoldi, C. (2008) Application of Brazilian-pine fruit coat as a biosorbent to removal of reactive red 194 textile dye from aqueous solution. Kinetics and equilibrium study. *J. Hazard. Mater.*, *155*: 536.
32. Largegren, S. (1898) About the theory of so-called adsorption of soluble substances. *Kungliga Suensk Vetenskapsakademiens Handlingar*, *241*: 1.
33. Ho, Y.S.; Mckay, G.M. (1999) Pseudo-second order model for sorption process. *Proc. Biochem.*, *34*: 451.
34. Perez-Marin, A.B.; Meseguer-Zapata, V.; Ortuño, J.F.; Aguilar, M.; Sáes, J.; Lloréns, M. (2007) Removal of cadmium from aqueous solutions by adsorption onto orange waste. *J. Hazard. Mater.*, *139*: 122.
35. Lopes, E.C.N.; dos Anjos, F.S.C.; Vieira, E.F.S.; Cestari, A.R. (2003) An alternative Avrami equation to evaluate kinetic parameters of the interaction of Hg(II) with thin chitosan membranes. *J. Colloid Interface Sci.*, *263*: 542.

36. Weber-Junior., W.J.; Morris, J.C. (1963) Kinetics of adsorption on carbon from solution. *J. Sanit. Eng. Div. Am. Soc. Civil Eng.*, *89*: 31.
37. Guo, B.; Hong, L.; Jiang, H.X. (2003) Macroporous poly(calcium acrylate-divinylbenzene) bead – a selective orthophosphite sorbent. *Ind. Eng. Chem. Res.*, *42*: 5559.
38. Langmuir, I. (1918) The adsorption of gases on plane surfaces of glass, mica and platinum. *J. Am. Chem. Soc.*, *40*: 1361.
39. Freundlich, H.M.F. (1906) Über die adsorption in lösungen. *Zeitschrift für Physikalische Chemie (Leipzig)*, *57A*: 385.
40. Sips, R. (1948) On the structure of a catalyst surface. *J. Chem. Phys.*, *16*: 490.
41. Redlich, O.; Peterson, D.L. (1959) A useful adsorption isotherm. *J. Phys. Chem.*, *63*: 1024.
42. Turan, P.; Doğan, M.; Alkan, M. (2007) Uptake of trivalent chromium ions from aqueous solutions using kaolinite. *J. Hazard. Mater.*, *148*: 56.
43. El-Sikaily, A.; El-Nemr, A.; Khaled, A.; Abdelwehab, O. (2007) Removal of toxic chromium from wastewater using green alga Ulva lactuca and its activated carbon. *J. Hazard. Mater.*, *148*: 216.
44. Mungasavalli, D.P.; Viraraghavan, T.; Jin, Y.C. (2007) Biosorption of chromium from aqueous solutions by pretreated Aspergillus niger: Batch and column studies. *Colloids Sur. A*, *301*: 214.
45. Bishnoi, N.R.; Kumar, R.; Kumar, S.; Rani, S. (2007) Biosorption of Cr(III) from aqueous solution using algal biomass spirogyra spp. *J. Hazard. Mater.*, *145*: 142.
46. Mohan, D.; Chander, S. (2006) Single, binary, and multicomponent sorption of iron and manganese on lignite. *J. Colloid Interface Sci.*, *299*: 76.
47. Gurnani, V.; Singh, A.; Venkataramani, B. (2003) Cellulose based macromolecular chelator having pyrocatechol as an anchored ligand: Synthesis and applications as metal extractant prior to their determination by flame atomic absorption spectrometry. *Talanta*, *61*: 889.
48. Öztaş, N.A.; Karabakan, A.; Topal, Ö. (2008) Removal of Fe(III) ion from aqueous solution by adsorption on raw and treated clinoptilolite samples. *Microporous Mesoporous Mater.*, in press. doi:10.1016/j.micromeso.2007.07.030.
49. Dimirkou, A. (2007) Uptake of Zn^{2+} ions by a fully iron-exchanged clinoptilolite. Case study of heavily contaminated drinking water samples. *Water Res.*, *41*: 2763.
50. Mendil, D.; Tuzen, M.; Soylak, M. (2008) A biosorption system for metal ions on Penicillium italicum – loaded on Sepabeads SP 70 prior to flame atomic absorption spectrometric determinations. *J. Hazard. Mater.*, in press. doi:10.1016/j.jhazmat.2007.07.097.
51. Veli, S.; Alyüz, B. (2007) Adsorption of copper and zinc from aqueous solutions by using natural clay. *J. Hazard. Mater.*, *149*: 226.
52. Amuda, O.S.; Giwa, A.A.; Bello, I.A. (2007) Removal of heavy metal from industrial wastewater using modified activated coconut shell carbon. *Biochem. Eng. J.*, *36*: 174.

53. Sales, J.A.A.; Petrucelli, G.C.; Oliveira, F.J.V.E.; Airoldi, C. (2007) Mesoporous silica originating from a gaseous ammonia epoxide ring opening and the thermodynamic data on some divalent cation adsorptions. *J. Colloid Interface Sci.*, *315*: 426.
54. Li, X.; Tang, Y.; Cao, X.; Lu, D.; Luo, F.; Shao, W. (2008) Preparation and evaluation of orange peel cellulose adsorbents for effective removal of cadmium, zinc, cobalt and nickel. *Colloids Surfaces A*, *317*: 512.
55. Incharoensakdi, A.; Kitjaharn, P. (2002) Zinc biosorption from aqueous solution by a halotolerant cyanobacterium *Aphanothece halophytica*. *Curr. Microbiol.*, *45*: 261.